

# Structural Characterization and Emulsifying Properties of a Water-Soluble *Buchanania lanzan* Gum Polysaccharide

Saptarshi Samajdar, K. Jayaram Kumar

Department of Pharmaceutical Sciences and Technology, Birla Institute of Technology, Mesra, Ranchi, Jharkhand, India

Submitted: 23-Feb-2022

Revised: 26-Feb-2022

Accepted: 16-Mar-2022

Published: 07-Jul-2022

## ABSTRACT

**Background:** *Buchanania lanzan* gum, better known as chironji gum, has been traditionally used as a binder in food preparations. Water-soluble polysaccharides have good emulsifying properties, but the polysaccharide structure elucidation of water soluble chironji gum has not been carried out, and also, its use in emulsion has not been explored. **Objectives:** The aim of this study is to perform structural characterization of water-soluble polysaccharide isolated from chironji gum (CGPS) and explore its nanoemulsifying properties. **Materials and Methods:** The water-soluble polysaccharide CGPS was isolated and fractionated by Sepharose 6B column. Structural characterization was investigated by high-performance liquid chromatography (HPLC), nuclear magnetic resonance (NMR), and gas chromatography–mass spectrometry (GC–MS). CGPS-stabilized nanoemulsion was formulated using Miglyol 812, Cremophor RH40, and diclofenac sodium and was evaluated. **Results:** The polysaccharide fraction had a yield of  $33.85\% \pm 0.88\%$  w/w. HPLC analysis revealed that CGPS consisted of galactose, rhamnose, arabinose, and glucose. CGPS had an average molecular weight of 201 kDa. Analytical studies, including NMR and GC–MS, showed that CGPS had repeating units of  $\rightarrow 4)\text{-}\alpha\text{-D-Galp}(1 \rightarrow 2)\text{-}\alpha\text{-L-Rhap}(1 \rightarrow$  with terminal  $\beta\text{-D-Glcp}(1 \rightarrow$  and  $\alpha\text{-L-Araf}(1 \rightarrow$  residues. The nanoemulsions prepared with CGPS showed a droplet size ranging from  $31.41 \pm 0.26$  to  $65.30 \pm 0.21$  nm, and negative zeta potential values were obtained for all the nanoemulsions. *In vitro* drug release studies of the CGPS nanoemulsion formulation revealed that diclofenac sodium release was delayed in simulated colonic fluid. **Conclusion:** This study indicates immense potential of CGPS for colon-targeted drug delivery system.

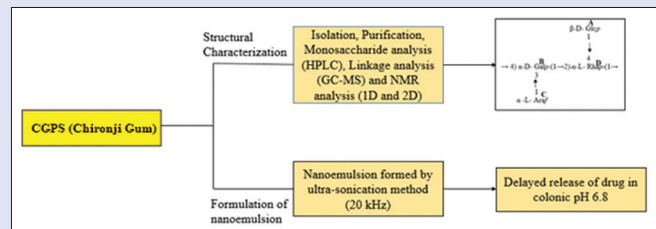
**Key words:** Chironji Gum, GC–MS, nanoemulsions, NMR spectroscopy, polysaccharide

## SUMMARY

- A water-soluble polysaccharide (CGPS) was isolated from chironji gum.
- Structural characterization of CGPS was studied by means of HPLC, NMR,

FTIR, and gas chromatography–mass spectrometry (GC–MS).

- CGPS has repeating units consisting of  $\rightarrow 4)\text{-}\alpha\text{-D-Galp}(1 \rightarrow 2)\text{-}\alpha\text{-L-Rhap}(1 \rightarrow$ .
- Side chains are composed of terminal  $\beta\text{-D-Glcp}(1 \rightarrow$  and  $\alpha\text{-L-Araf}(1 \rightarrow$  residues.
- Nanoemulsions prepared with CGPS demonstrated delayed drug release at the site of colon.



**Abbreviations used:** GPC: Gel permeation chromatography; DMSO: Dimethyl sulfoxide; TFA: Trifluoroacetic acid; USP: United States Pharmacopoeia; CGPS: Chironji gum polysaccharide; HPLC: High-performance liquid chromatography; NMR: Nuclear magnetic resonance;  $^1\text{H}$  NMR: Proton NMR;  $^{13}\text{C}$  NMR: Carbon NMR; FTIR: Fourier transform infrared spectroscopy; GC–MS: Gas chromatography–mass spectrometry; PMP: 1-Phenyl-3-methyl-5-pyrazolone; HCl: Hydrochloric acid; NaOH: Sodium hydroxide; ppm: Parts per million; PMAA: per-methylated alditol acetates. d.b: dry basis; PDA: Photo Diode Array; GC: Gas Chromatography

## Correspondence:

Dr. K. Jayaram Kumar,  
Department of Pharmaceutical Sciences and  
Technology, Birla Institute of Technology, Mesra,  
Ranchi - 835 215, Jharkhand, India.  
E-mail: jayarampharm@gmail.com  
**DOI:** 10.4103/jpm.pm\_96\_22

## Access this article online

Website: www.phcog.com

## Quick Response Code:



## INTRODUCTION

Nanoemulsion drug delivery systems have proven to be promising tools in improving bioavailability of drug and bioactive food and targeted drug delivery in critical diseases like brain carcinoma and inflammations in colon. Lipid-based nanoemulsion formulations are now a suitable option for delivering medication and bioactive food components with low oral bioavailability and other formulation issue.<sup>[1]</sup> However, synthetic emulsifying agents can cause irritations and toxicity. So, plant polysaccharides can be used as an adjuvant to deal with this problem. Plant polysaccharides are complex biopolymers which have attracted scientists all over the world for years, due to their higher degree of biocompatibility, renewability, and biodegradability.<sup>[2]</sup> Some of the polysaccharides have been traditionally used for various clinical purposes as well as in drug delivery. Different functional groups can be observed in the structure of polysaccharides from different sources and they display different physico-chemical properties. These properties make them suitable for different food and pharmaceutical applications,

especially in drug delivery systems. Most of the polysaccharides are preferred over their synthetic counterparts due to being inexpensive, abundant availability, and non-toxic nature.<sup>[3]</sup>

Chironji (*Buchanania lanzan* Spreng.) of the Anacardiaceae family, locally known as Cudappa almond or piyal, is an evergreen tree native to the deciduous forests of Jharkhand, Chhattisgarh, and Madhya Pradesh that can be a good source of plant polysaccharide. Its flat

This is an open access journal, and articles are distributed under the terms of the Creative Commons Attribution-NonCommercial-ShareAlike 4.0 License, which allows others to remix, tweak, and build upon the work non-commercially, as long as appropriate credit is given and the new creations are licensed under the identical terms.

**For reprints contact:** WKHLRPMedknow\_reprints@wolterskluwer.com

**Cite this article as:** Samajdar S, Kumar KJ. Structural characterization and emulsifying properties of a water-soluble *Buchanania lanzan* gum polysaccharide. Phcog Mag 2022;18:418-26.

lentil-sized seeds are often consumed raw or roasted. It is recognized to be extremely nutritious, with 43.2% protein, 38% fat, and a high calorific value (230 kcal). It has also been discovered to have medicinal value. Its gum, which has traditionally been employed as a food binder, stabilizer, bioadhesive, and thickening for food, can also be used as an excipient in solid dosage form as a rich food and medicinally important plant. This also reduces the potential for toxicity when used as excipients. The plant's bark produces a large amount of gum exudate. Several gums have been extensively studied for various food additives, natural emulsifiers or stabilizers, as well as pharmaceutical excipients for various drug delivery systems, such as gum katira, zedo gum, and erasmus.

*Buchanania* genus has 26 species around the world and was first discovered in the Polynesian island of Papua New Guinea. In India, *Buchanania lanceolata* and *B. lanzan* are native. The bark exudate of *B. lanzan* is thick reddish or yellowish colored hard mass that is soluble in water. However, the detailed structure of polysaccharide was not established.<sup>[4]</sup>

The current study focuses on the robust purification of chironji gum polysaccharide, structural characterization, and its nanoemulsifying properties.

## MATERIALS AND METHODS

### Materials

The authenticated gum sample of chironji gum was procured from a local forest from the Indian Institute of Natural Gums and Resins, Namkum, Ranchi, Jharkhand, India. Hi-Media Ltd provided us with standard monosaccharides (arabinose, galactose, glucose, mannose, rhamnose, and xylose). Cellulose membrane with retention of MW > 12 kDa and AR grade trifluoroacetic acid (TFA) were purchased from (Sigma Aldrich, Missouri, USA). All the other chemicals used were of analytical grade.

### Isolation and Purification of Gum

Ten grams of crushed gum was sieved in 60 mesh and cooked for 6 h (at 80°C) in 500 mL deionized water. The dispersion was filtered using muslin cloth after cooling at 4°C overnight. The filtered dispersion was centrifuged for 25 min at 3500 rpm (R-8C; Remi, Mumbai, India). The residue debris was discarded, while the supernatant was concentrated, and 95% ethanol was used to precipitate the concentrated supernatant in a 1:5 v/v ratio. The precipitate was recovered by centrifugation (3500 rpm for 25 min) and it was dialyzed with cellulose membrane (Sigma-Aldrich; retaining > MW 12 kDa) for removal of low-molecular-weight material after 12 h of storage at 4°C.<sup>[5]</sup> The aqueous dialyzed dispersion was collected and lyophilized to give crude polysaccharide, CGP.

The isolated crude polysaccharide CGP (25 mg) was diluted in 10 mL deionized water and purified using gel permeation chromatography (GPC) on a Sepharose 6B (10,000–1,000,000 Da) 90 cm × 2.1 cm column and water as the eluent (0.4 mL/min). Forty-eight test tubes (4 mL each) were collected and lyophilized to obtain the purified polysaccharide, CGPS. The fractions were analyzed for their sugar content spectrophotometrically at 490 nm using phenol–sulfuric acid reagent (UV 2450; Shimadzu, Kyoto, Japan).<sup>[6]</sup>

### Physico-chemical Properties

#### Solubility and swelling index

The swelling ability and solubility of CGPS can be measured using the method described by Varma, *et al.* (2014) with minor modifications. The isolated CGPS sample ( $W_i$ ) was added to distilled water (1% w/w). The sample was heated on a shaking water bath (Remi, Mumbai, India) at various temperatures for 30 min with constant stirring. It was brought

to room temperature and centrifuged for 15 min at 3000 rpm. Each sample's supernatant was thoroughly decanted. The weight of the swelled polysaccharide residue ( $W_{ss}$ ) was recorded. The supernatant ( $W_{su}$ ) was dried for 12 h at 50°C in a hot air oven.<sup>[7]</sup>

$$\% \text{Solubility} = \left( \frac{W_{su}}{W_i} \right) \times 100$$

$$\% \text{Swelling} = \left( \frac{W_{ss}}{W_i \times (100 - \% \text{solubility})} \right) \times 100$$

Where  $W_i$  is the initial weight of the sample.

#### Effect of pH on solubility

The effect of pH on solubility was determined by preparation of 1% w/v dispersion of CGPS in distilled water and pH was adjusted with 0.1 M HCl and 0.1 M NaOH to the desired values of pH 1.2 and pH 6.8. The dispersions were allowed to stand for 30 min at room temperature before being centrifuged for 10 min at 3000 rpm. The solubility of the supernatant was measured by observing it in specific pH ranges, as described above.<sup>[8]</sup>

#### Water-holding capacity

One hundred milligrams of CGPS ( $W$ ) was hydrated in 10 mL water and stirred for 1 h at room temperature with a magnetic stirrer. The resulting sample was centrifuged for 15 min at 3000 rpm. The supernatant was discarded, and the residue weight ( $W_s$ ) was determined.<sup>[9]</sup>

$$\text{WHC} = \left( \frac{W_s - W}{W} \right) \times 100$$

#### Moisture content

Then, 0.5 g of polysaccharide CGPS was taken in an aluminum moisture cup. It was placed in an oven at 105°C until constant weight of the sample was obtained.<sup>[10]</sup>

#### Morphological study

A field emission scanning electron microscope (Zeiss Gemini Instrument, Jena, Germany) with a 1 kV accelerating voltage was used to examine the surface morphology of CGPS. The sample was coated with gold and put to an aluminum stub with conductive carbon double tape. The images were captured under magnifications of 200 × and 500 ×.

#### Fourier transform infrared spectroscopy analysis

The Fourier transform infrared spectroscopy (FTIR) spectrum was recorded in an FTIR spectrometer (FTIR-8400S; Shimadzu, Japan) with the wavelength ranging between 4000 and 600  $\text{cm}^{-1}$ . The sample (10 mg) and KBr (250 mg) were precisely weighed and blended, and the data were collected with FTIR.

#### Estimation of molecular weight

The molecular weight of CGPS was estimated by GPC using dextrans (T 400, T 275, T 200, T 70, and T 40). The sample and the reference dextrans were eluted using the Sepharose 6B column having a total volume of 1246.2  $\text{cm}^3$ . The total sugar content of the collected samples was determined using a phenol–sulfuric acid assay at 490 nm (Shimadzu UV 2450; Shimadzu, Japan). The elution volumes of standards were plotted in a graph against their respective molecular weights. Molecular weight of CGPS was estimated by plotting the elution volume of CGPS polysaccharides in the same graph.<sup>[11]</sup>

#### Monosaccharide composition analysis

Reverse-phase high-performance liquid chromatography (HPLC) method was used for estimation of monosaccharide composition of CGPS polysaccharides. Fifty milligrams Dry basis (d.b.) of CGPS

polysaccharide was added to 3 mL of 3 M TFA and incubated at 120°C for 2 h. Excess TFA was removed under reduced pressure by rota evaporation, and then small amount of methanol was added to remove residual TFA. Then, 100 µL of hydrolyzed CGPS dispersion was labeled with 0.5 M methanolic 1-phenyl-3-methyl-5-pyrazolone (PMP) (50 µL) and 50 µL of 0.3 M NaOH. At 70°C, the mixture was reacted for 1 h and was brought to room temperature and neutralized with 0.3 M HCl. Then, the sample was centrifuged at 2000 rpm for 5 min. The supernatant was filtered using 0.22 µm nylon filter. The above PMP-labeled polysaccharide hydrolysate was analyzed using HPLC system (Waters, Massachusetts, USA) consisting of C<sub>18</sub> Spherisorb column (4.6 mm × 250 mm) and a Photo Diode Array (PDA) detector. Acetonitrile and 0.1 M phosphate buffer (17:83) were used as the mobile phase with a flow rate of 1 mL/min. The qualitative and quantitative estimation of monosaccharides was performed by comparing with standard monosaccharide units like arabinose, glucose, galactose, mannose, rhamnose, and xylose. The molar ratio of the sugars present was calculated from the peak area of the chromatogram. The measurement of uronic acid was performed by *m*-hydroxydiphenyl method.<sup>[12]</sup>

### NMR spectroscopy

The isolated CGPS sample (25 mg d.b.) was solubilized in 99% deuterium oxide. <sup>1</sup>H and <sup>13</sup>C spectra of the polysaccharide dispersion were recorded at 27°C on 400 MHz nuclear magnetic resonance (NMR) spectrometer (Jeol, Tokyo, Japan) with an assigned delay time of 2s. The chemical shifts are expressed in ppm unit.<sup>[13]</sup>

### Methylation analysis

The purified CGPS was subjected to methylation as per the method suggested by Ciucanu and Kerek (1984) with slight modifications. Twenty milligrams of dried CGPS sample d.b. was added to 3 mL of anhydrous dimethyl sulfoxide (DMSO) and heated at 60°C to dissolve it. Then, 50 mg of finely powdered NaOH was added under constant stirring and reacted for 60 min in a sealed condition, followed by the addition of 1 mL of cold (4°C) methyl iodide. The reaction mixture was vortexed for 5 min.<sup>[14]</sup> After 1 h of reaction at room temperature, the reaction was terminated by using water and the methylated product was isolated by partitioning between chloroform and water in a ratio of 3:2 (v/v). The organic layer containing the methylated product was washed with distilled water for many times and dried. The methylated product was examined by FTIR (FTIR-8400S; Shimadzu, Japan). The disappearance of O–H band between 3100 and 3400 cm<sup>-1</sup> confirms methylation. The dried, methylated CGPS (20 mg) was hydrolyzed in 3 mL of 3 M TFA in a sealed flask for 2 h at 120°C. Under reduced pressure, excess TFA was removed, and then, in the reaction mixture, small amount of methanol was added for the removal of residual TFA. The hydrolyzed sample of CGPS was reduced using NaBH<sub>4</sub> and acetylated with acetic anhydride and pyridine in a ratio of 1:1.<sup>[15]</sup> Then, the partially methylated alditol acetates were analyzed by gas chromatography–mass spectrometry (GC–MS) apparatus (Perkin Elmer Clarus 600; Perkin Elmer; Massachusetts; United States.) equipped with 30 m × 0.25 mm × 0.25 µm HP-5 fused silica capillary columns. The initial temperature of the column was set up at 150°C (2 min) at a flow gradient of 4°C/min, up to a final temperature of 200°C. Helium was used as the carrier gas.<sup>[16]</sup>

## Formulation of Oil in Water Nanoemulsion

### Screening of oils and surfactants

Screening of oils and surfactants was performed as reported by Azeem *et al.*<sup>[17]</sup> (2009) with slight modifications. Solubility of the model drug diclofenac sodium in different oils and stabilizing surfactant agent was determined by addition of an extra amount of drug in a capped vial containing 2 mL of the vehicle. The dispersion was heated at 37°C

under continuous agitation for 24 h. After equilibrium was reached, each of the vials was centrifuged at 3000 rpm for 15 min, with excess diclofenac sodium filtered using 0.45 µm membrane filter. The drug concentration was determined by measuring the absorbance at 276 nm using UV–Visible spectrophotometer (UV2450; Shimadzu, Japan).<sup>[18]</sup>

### Preparation of polysaccharide-based nanoemulsions

The oil in water (o/w) nanoemulsion was formulated based on the methods used by Ghosh *et al.*<sup>[19]</sup> (2013) with slight modifications [Figure 1]. The nanoemulsion was formulated using aqueous phase titration method. Miglyol 812, which is considered safe for pharmaceutical formulation, was selected as the oil phase after screening for the present research due to its maximum drug solubilization capacity (50.49 ± 0.06 mg/mL). Cremophor RH40 was used as the surfactant for its solubilization capacity of 50.79 ± 0.11. Initially, primary emulsion was prepared by addition of the organic phase containing mixture of oil and surfactant in the same ratio of 1:4 (v/v) to water phase consisting of 0%, 2.5%, and 5% water-soluble CGPS polysaccharide using a magnetic stirrer at 500 rpm (CF1, CF2, and CF3) [Table 1]. The primary emulsions CF1, CF2, and CF3 were then subjected to ultrasonic emulsification in a 20 kHz sonicator (PCI analytics, Thane, India). The sonicator generated disruptive forces, providing acoustic streaming and cavitation which reduced the droplet size from coarse emulsion to nanoemulsion.<sup>[20]</sup>

## Evaluation of Nanoemulsion

### Droplet size determination

The droplet size of CF1, CF2, and CF3 was measured using Zetasizer (Nano ZS; Malvern Instruments, Worcestershire, UK) at 25°C, which was based on dynamic light scattering technique. The samples were diluted 50 times using distilled water before the experiment for prevention of multiple light scattering.<sup>[21]</sup>

### Measurement of zeta potential

The zeta potential of the nanoemulsions was determined by nano laser particle size analyzer (Nano ZS, Malvern Instruments) at 25°C. For

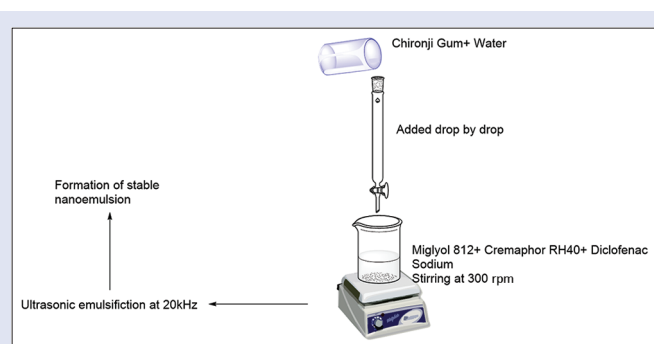


**Figure 1:** Schematic depiction of the protocol for the chironji gum nanoemulsion preparation

**Table 1:** Composition of all the nanoemulsion formulations

Phase	Constituents	CF1 (%w/w)	CF2 (%w/w)	CF3 (%w/w)
Oil phase	Miglyol 812	10	10	10
	Cremophor RH40	2.5	2.5	2.5
	Diclofenac sodium	0.1	0.1	0.1
Aqueous phase	Distilled water	87.4	84.9	82.4
	CGPS	0	2.5	5

CGPS=chironji gum polysaccharide

avoidance of multiple scattering effects and for distribution of size, the emulsions were diluted 50 times using distilled water under constant agitation.<sup>[22]</sup>

### Emulsion stabilities

The physical stability of chironji gum-based nanoemulsions was evaluated for 30 days at 25°C using Zetasizer (Nano ZS, Malvern Instruments) equipped with the multiple light scattering technique. Stability of emulsion stability was studied by analyzing the droplet size and zeta potential.<sup>[23]</sup>

### In vitro dissolution

*In vitro* release study was performed separately in 900 mL of pH 1.2 HCl solution for the first 60 min and pH 6.8 phosphate buffer for the next 300 min using an eight-station dissolution apparatus (L8000; LabIndia; Mumbai, India). Using the United States Pharmacopoeia (USP) II method, 10 mL of each of the CF1, CF2, and CF3 formulations (dose containing 10% diclofenac sodium) was placed in individual dialysis membranes with a cut-off of 12 kDa. The dialysis membranes were soaked in distilled water for 6 h before the *in vitro* dissolution study. Five milliliters of the sample was withdrawn from each of the stations at time intervals of 30 min up to 360 min and was simultaneously replenished with the same amount of fresh dissolution media for maintenance of the sink condition. Analyses of the samples were performed using UV-Visible spectrophotometer (model UV-2450; Shimadzu, Japan) at 276 nm. The drug release data was used to calculate the % dissolution efficiency.<sup>[9,24,25]</sup>

### Statistical Analysis

All the data reported are an average of triplicate observations. The data are expressed as mean  $\pm$  standard deviation.

## RESULTS

### Physico-chemical Characteristics of CGPS

In terms of yield, water-binding capacity, moisture content, solubility, and swelling power, physico-chemical parameters of CGPS were assessed. The overall percentage yield of CGPS was found to be 33.85%  $\pm$  0.88% w/w. CGPS was determined to have a moisture content of 0.71%  $\pm$  0.02% w/w. In formulations containing hygroscopic medications, low moisture is optimal.<sup>[26,27]</sup> Water-holding capacity of CGPS was 143.15%  $\pm$  0.76%, suggesting its uses in granulation and in maintaining the physical integrity and stability of solid oral dosage forms, thereby modifying its texture and preventing flaws.<sup>[28,29]</sup>

The solubility and swelling power of CGPS dispersion at different temperatures (30°C–90°C) ranged between 94.7%  $\pm$  0.02%–99.1%  $\pm$  0.05% and 2.39%  $\pm$  0.01%–4.43%  $\pm$  0.06%, respectively, with respect to the weight of CGPS taken for their determination. The lower swelling has been attributed to higher degree of intermolecular associations of the polysaccharide, finding its application in controlled release drug delivery.<sup>[30]</sup> The solubility of CGPS increased steadily from pH 1.2 to pH 6.8, implying that solubility increases as the pH rises from pH 1.2 to phosphate buffer pH (pH 6.8). This reveals that the solubility of CGPS is pH dependent.<sup>[8]</sup>

### Morphological Property of CGPS

Under 200 $\times$  and 500 $\times$  magnification, the scanning electron microgram of CGPS in Figure 2 shows aggregates of randomly distributed, irregularly shaped polysaccharide with smooth surface and some crevices. The irregularly shaped particles indicate that it is amorphous. The crevices on the surface of CGPS aid in drug entrapment and delayed release of drug.<sup>[31]</sup>

### FTIR Analysis of CGPS

FTIR spectrum [Figure 3] of CGPS is broadly used to reveal the presence of main functional groups in it. The spectrum revealed typical major broad peak between 3100 and 3400  $\text{cm}^{-1}$ , which was characteristic of O–H stretching, as well as a small sharp band around 2946  $\text{cm}^{-1}$ , attributed to C–H stretching band of  $\text{CH}_2$  groups.<sup>[32]</sup> The absorption bands at 1613 and 1677  $\text{cm}^{-1}$  were responsible for interchain interaction. An absorption band at 1405  $\text{cm}^{-1}$  is assigned to deforming vibration of the C–H bond.<sup>[33]</sup> Polysaccharides have the fingerprint region 900–1300  $\text{cm}^{-1}$ , by which the functional groups can be identified. The pyranose form of sugar was responsible for the absorption at 1044 and 1126  $\text{cm}^{-1}$ . The presence of both  $\alpha$  and  $\beta$  polysaccharides in the structure is indicated by the band at 829 and 870  $\text{cm}^{-1}$ . According to the findings, CGPS is a neutral polysaccharide with both  $\alpha$  and  $\beta$  configuration units.<sup>[34,35]</sup>

### Molecular Weight and Monosaccharide Composition of CGPS

The polysaccharide CGPS was fractionated through Sepharose 6B column for estimation of molecular weight. The elution profile of purified CGPS showed a single symmetrical peak, which indicated CGPS to be one homogenous fraction [Figure 4], as detected by phenol-sulfuric acid assay. The fractions in tube 12–28 were pooled together and used for the estimation of molecular weight.<sup>[36,37]</sup> The molecular weight of CGPS was estimated to be around 201 kDa based on the calibration curve prepared with standard dextrans.<sup>[38]</sup> The chromatogram of isolated CGPS sample had four distinct PMP-labeled monosaccharide peaks present, which were separated from each other. By comparison with chromatograms of the mixture of standard monosaccharides, the monosaccharide residues present in CGPS were identified as galactose, rhamnose, arabinose, and glucose and from the peak area, their molar ratio was estimated to be about 1.02:1.05:1.02:1.00. No uronic acid was detected in polysaccharide CGPS by *m*-hydroxydiphenyl method, with d-glucuronic acid being used as the standard.

### Structural Characterization of CGPS

#### Methylation analysis

The GC-MS analysis of the methylated products is summarized in Table 2. The per-methylated alditol acetates (PMAA) of CGPS were composed of four monosaccharide units, namely, 2,6-Me<sub>2</sub>-Galp and 3-Me-Rhap, 2,3,5-Me<sub>3</sub>-Araf, and 2,3,4,6-Me<sub>4</sub>-Glc, at a molar ratio of about 25:25:25:25. They were identified by comparing with standard derivatives. The results from the analysis were consistent with monosaccharide analysis demonstrating the presence of (1  $\rightarrow$  3,4)-linked Galp and (1  $\rightarrow$  2,4)-linked Rhap as the major components of repeating unit with terminal Glcp and Araf moieties distributed in branches.<sup>[39]</sup>

### NMR Spectroscopy Analysis

The proton and carbon spectra are shown in Figure 5a and b, respectively. The anomeric protons of B (5.24), C (5.24), and D (5.00) had chemical shift larger than 5 ppm, suggesting them to be  $\alpha$  linked, while residue A (4.51) had a chemical shift between 4 and 5 and a large coupling constant suggested that it is a  $\beta$ -linked monosaccharide residue. The carbon spectrum presented in Figure 5b contained four signals at anomeric region  $\delta$  103.96, 99.06, 109.77, and 103.10. Hence, the residues were identified as  $\beta$ -d-glucopyranose (A),  $\alpha$ -d-galactopyranose (B),  $\alpha$ -l-arabinofuranose (C), and  $\alpha$ -l-rhamnopyranose (D). All the signals of carbon and proton NMR were confirmed by 2D NMR analysis. All the results confirmed the presence of four sugar residues consistent with: Gas Chromatography (GC) and FTIR data. The signals at  $\delta$  1.08/15.45 were due to the H-6/C-6 of residue D, and high value of  $\delta$  109.77 indicates

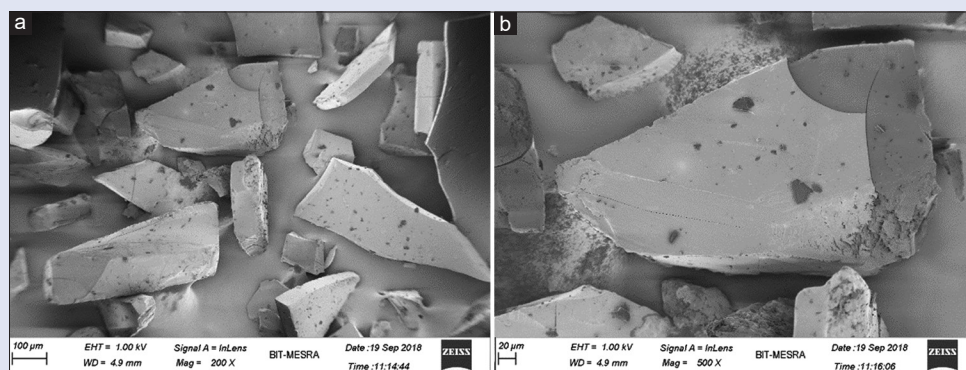


**Figure 2:** Field Emission Scanning Electron Microscope (FESEM) images of piyal gum polysaccharide: (a) 200 × and (b) 500×

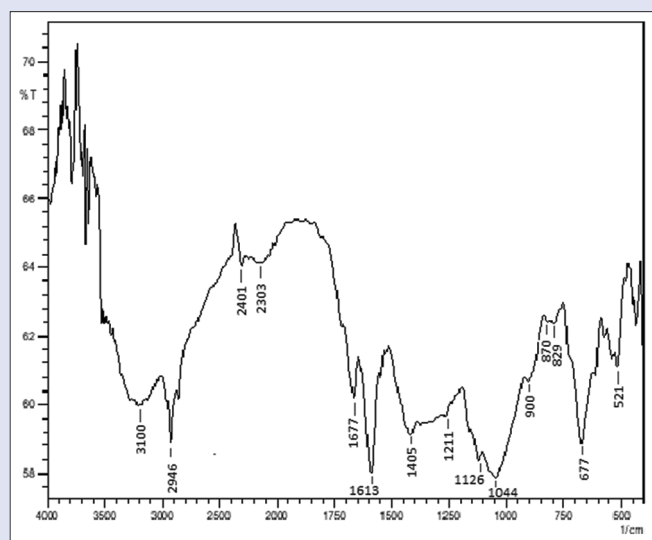


**Figure 3:** FTIR spectrum of isolated polysaccharide from piyal gum (CGPS). CGPS = chironji gum polysaccharide, FTIR = Fourier transform infrared spectroscopy

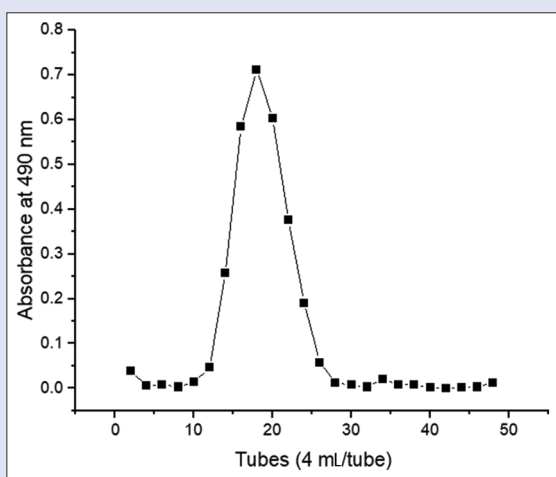


**Figure 4:** Elution profile of CGPS, obtained by gel permeation chromatography. CGPS = chironji gum polysaccharide

$\alpha$ -linked C-1 of residue C. All the NMR chemical shifts [Table 3] were compared with the literature values.<sup>[40,41]</sup>

In view of the above results, the structure of water-soluble polysaccharide from chironji gum (CGPS) is proposed below [Figures 6 and 7].

The reported structure of polysaccharide CGPS was found to contain residues of rhamnose and galactose in its repeating unit, which are known to have a strong tendency to aggregate in solution depending on the method of extraction and concentration.<sup>[42,43]</sup>

## Evaluation of Nanoemulsion

### Solubility studies

Pure diclofenac sodium was reported to be poorly soluble in water.<sup>[44]</sup> The solubility of the drug in various oils and surfactants is shown in Table 4. Diclofenac sodium was quite soluble in selected oils, with the highest solubility observed in Miglyol 812 ( $50.79 \pm 0.18$  mg/mL) and the lowest in soy oil ( $14.58 \pm 0.11$  mg/mL), while among the surfactants, highest solubility was observed in Cremophor RH40 ( $50.49 \pm 0.15$  mg/mL) [Table 4]. Based on these results, Miglyol 812 and Cremophor RH40 were chosen as the oil phase and surfactant, respectively, for pure diclofenac sodium.<sup>[24,45]</sup>

### Droplet size measurement

The droplet size of chironji gum-based nanoemulsion formulations is shown in Figure 8. The droplet size of the formulation CF1 was found to be  $231.13 \pm 0.33$  nm, while  $65.30 \pm 0.21$  and  $31.41 \pm 0.26$  nm were the droplet sizes of CF2 and CF3, respectively. With increase in the concentration of chironji gum in the formulations, there was a significant drop in the droplet size. Smaller particle sizes were obtained at higher particle concentration of chironji gum because more particles are available to stabilize larger overall interfacial area.<sup>[46]</sup>

### Zeta potential measurement

Zeta potential measurement of all the gum-based formulations was found to be negative. The values of zeta potential were observed to be  $-16.73 \pm 0.06$ ,  $-30.68 \pm 0.19$ , and  $-36.24 \pm 0.08$  mV for CF1, CF2, and CF3, respectively. From Figure 9, it can be observed that there was a significant increase of zeta potential. Formulations with an increase in concentration of chironji gum showed an increase in negative charge of the emulsion, which, therefore, increased the negatively charged zeta potential as well. The aggregation of emulsion droplet was prevented due to higher electric charge on the surface of emulsion droplets because of the presence of strong repellent forces among droplets.<sup>[47]</sup>

### Stability studies of the emulsions

The stability of chironji gum nanoemulsions was evaluated by measurement of zeta potential and droplet size using laser diffraction scattering after 30 days of storage at room temperature. From Figure 10, it can be observed that the formulations CF1, CF2, and CF3 preserved their monomolar distribution. After 30 days, the formulations CF2 and

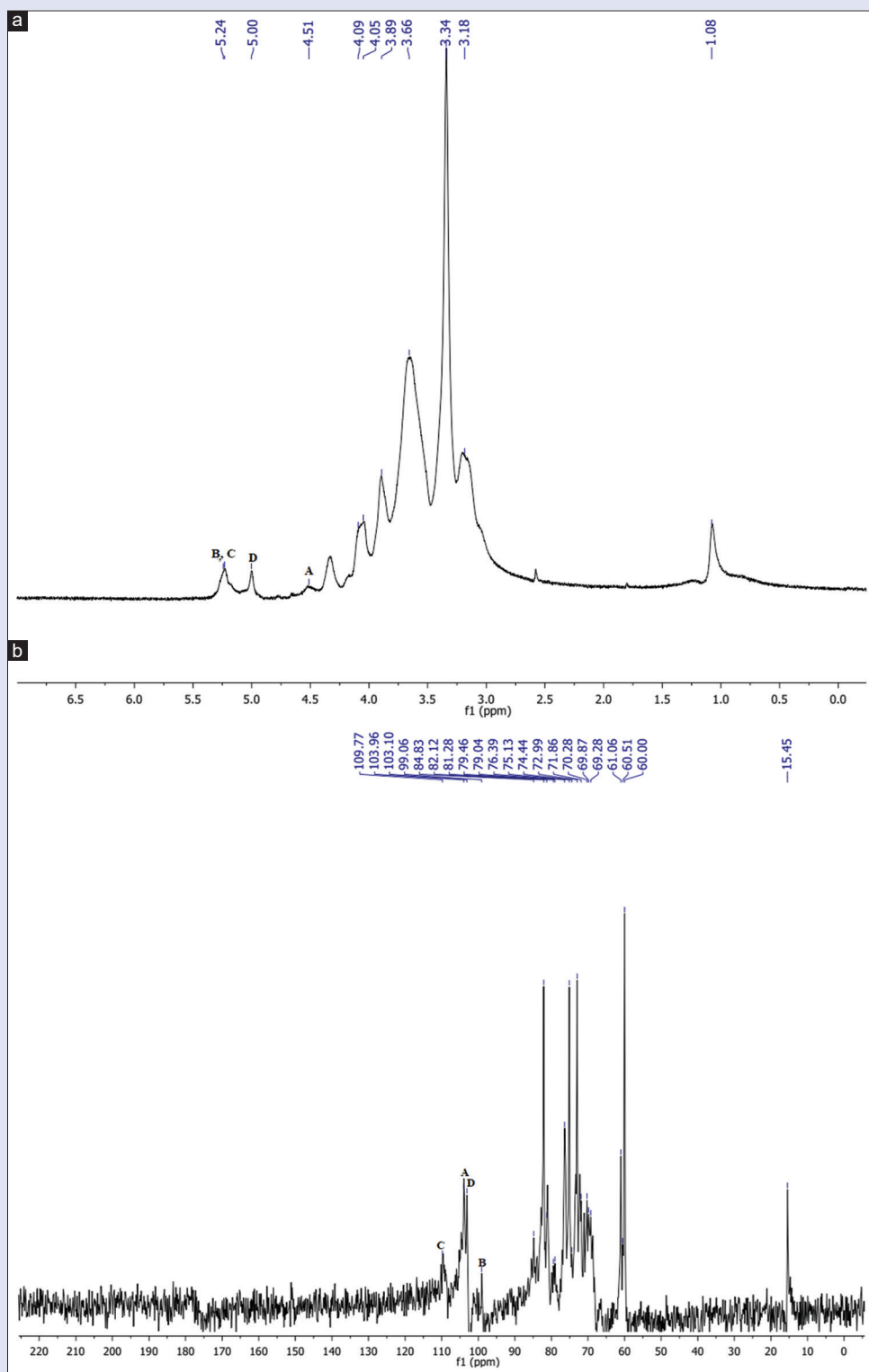


Figure 5: NMR spectra of CGPS: (a) <sup>1</sup>H NMR spectrum; (b) <sup>13</sup>C NMR spectrum. CGPS = chironji gum polysaccharide, NMR = nuclear magnetic resonance

Table 2: GC–MS data analysis of methylated alditol acetates of CGPS

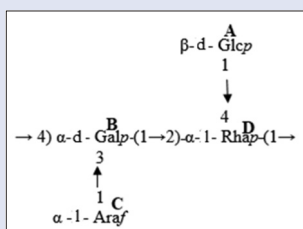
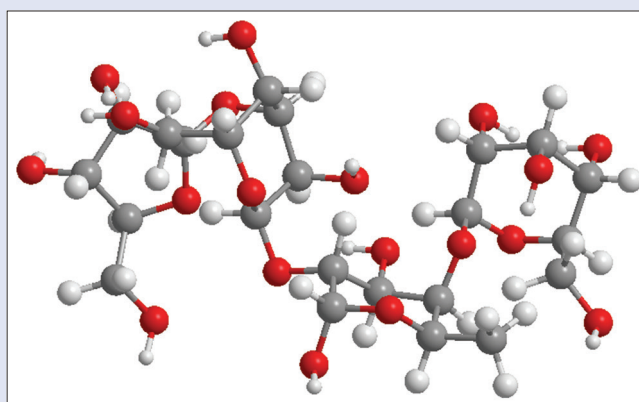
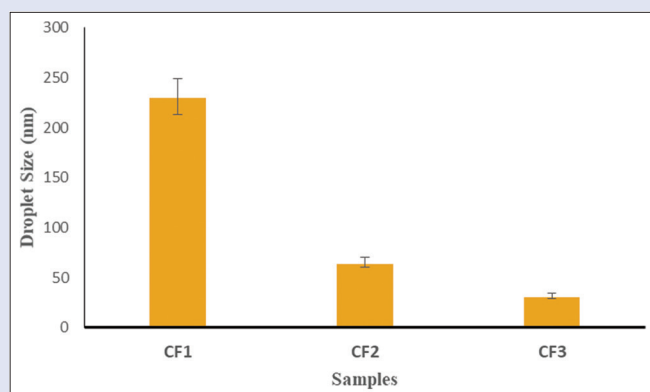
Methylated sugars	Mass fragments ( <i>m/z</i> )	Linkage pattern
2,3,5-Me <sub>3</sub> -Araf	45, 59, 71, 75, 102, 118, 129, 145, 161	Araf-(1→
2,3,4,6-Me <sub>4</sub> -GlcP	45, 71, 102, 118, 129, 145, 162, 189, 206, 280	GlcP-(1→
3-Me-Rhap	46, 74, 89, 100, 118, 131, 143, 160, 188, 206, 280	→2,4)-Rhap-(1→
2,6-Me <sub>2</sub> -GalP	45, 74, 87, 118, 129, 143, 161, 185, 232	→3,4)-GalP-(1→

CGPS=chironji gum polysaccharide, GC–MS=gas chromatography–mass spectrometry

**Table 3:** Chemical shift assignment for <sup>1</sup>H and <sup>13</sup>C NMR spectra of CGPS

Residues	C-1/H-1	C-2/H-2	C-3/H-3	C-4/H-4	C-5/H-5	C-6/H-6
β-d-Glucopyranose	103.96	70.28	74.44	72.99	75.13	61.06
α-d-Galactopyranose	4.51	3.69	4.05	3.36	3.66	3.66 (a) 3.88 (b)
α-d-Galactopyranose	99.06	69.87	84.83	81.07	71.86	60.51
α-l-Arabinofuranose	5.24	3.66	3.88	3.89	3.65	3.66 (a) 3.67 (b)
α-l-Arabinofuranose	109.77	79.46	76.39	79.04		-
	5.24	4.05	3.89	3.68	60.00	-
					3.68 (a) 4.09 (b)	
α-l-Rhamnopyranose	103.10	81.28	70.28	82.12	69.28	15.45
	5.00	4.09	3.34	3.18	3.38	1.08

CGPS=chironji gum polysaccharide, NMR=nuclear magnetic resonance

**Figure 6:** Predicted structure of CGPS. CGPS = chironji gum polysaccharide**Figure 7:** 3D model of the repeating units of CGPS. CGPS = chironji gum polysaccharide**Figure 8:** Droplet size distribution for nanoemulsions (CF1, CF2, and CF3)

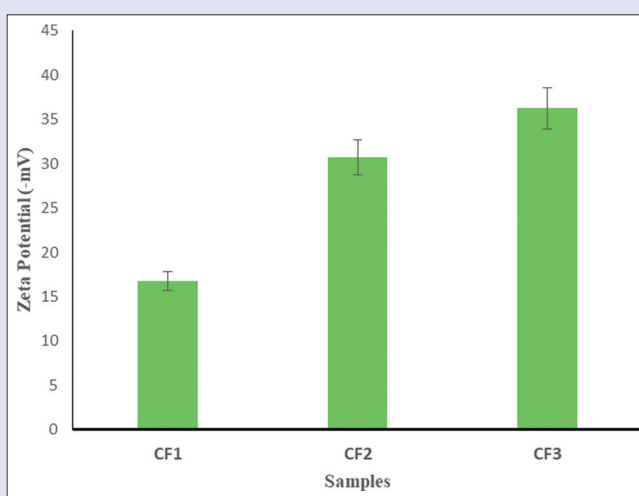
CF3 stabilized, with chironji gum showing smaller droplet size and higher zeta potential compared to CF1, which is in agreement with the previous values seen on the day of preparation.<sup>[48,49]</sup>

### In vitro drug release studies

*In vitro* dissolution studies were performed comparing the three formulations of nanoemulsion containing 10 mg of diclofenac sodium for a period of 6 h. All the formulations were found to be gastroresistant. The drug release of the nanoemulsion CP1 formulation prepared without chironji gum showed release of  $30.06 \pm 0.37$ , while the formulations CP2 and CP3 containing 2.5% and 5% w/w chironji gum, respectively, significantly delayed the release of  $25.11 \pm 0.28$  and  $11.71 \pm 0.31$ , compared to CP1 formulation [Figure 11]. It could be suggested that the release of drug is connected to the diffusion of small-sized droplets into the surrounding layer of chironji gum in the buffer medium, indicating its usage in colon-targeted delayed release of drugs.<sup>[50]</sup>

## CONCLUSION

In this study, a water-soluble polysaccharide (CGPS) with a molecular weight around 201 kDa, isolated from chironji gum,

**Figure 9:** Zeta potential of nanoemulsions (CF1, CF2, and CF3)

a readily available gum all over India, was used as an adjuvant in improving the availability of diclofenac sodium tablets. Investigation of structural features revealed that the linear chain consisted of  $\rightarrow 3,4$ -α-d-Galp-(1 → and  $\rightarrow 2,4$ -α-l-Rhap-(1 → attached in (1 → 2) positions. The terminal α-l-Araf and β-d-Glcp are attached to C-3 and C-4 of Galp and Rhap, respectively. The nanoemulsion formulations having droplet size ranging from  $65.30 \pm 0.21$  to  $31.41 \pm 0.26$  nm and zeta potential ranging between  $-30.68 \pm 0.19$  and  $-36.24 \pm 0.08$  mV demonstrated gastroresistant delayed drug release at the site of colon. This indicated immense potential of CGPS in delayed release of

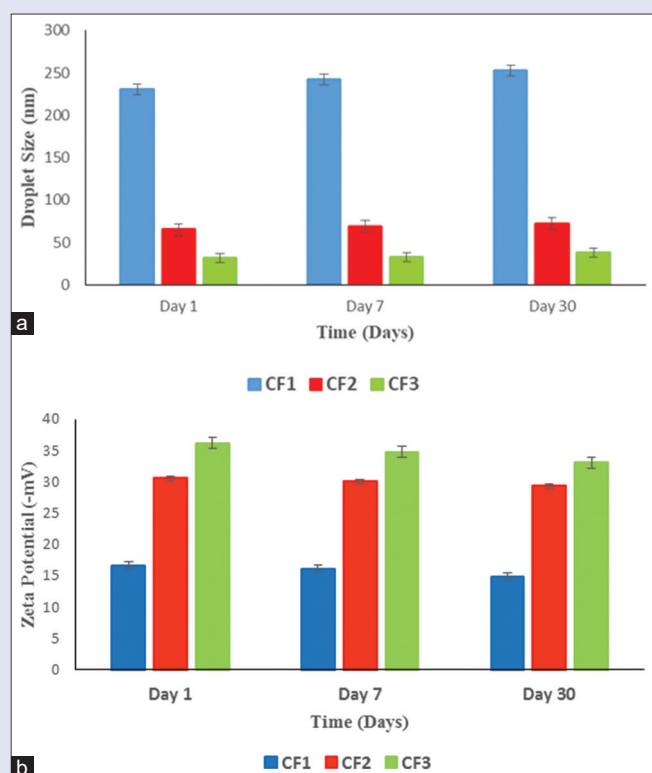


**Figure 10:** Droplet size (a) and zeta potential (b) of o/w nanoemulsions for three different emulsions (CF1, CF2, and CF3). o/w = oil in water

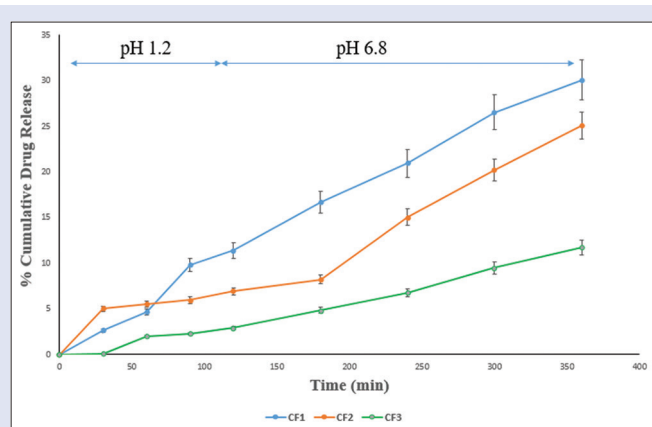


**Figure 11:** *In vitro* drug release profile of the drug from nanoemulsion formulations CF1, CF2, and CF3

**Table 4:** Solubility of diclofenac sodium in various oils and surfactants

Components	Category	Solubility (mg/mL)
Soy oil	Lipid	14.58±0.11
Nigella oil	Lipid	26.29±0.29
Miglyol 812	Lipid	50.79±0.18
Tween 20	Surfactant	40.68±0.23
Tween 80	Surfactant	38.59±0.33
Cremophor RH 40	Surfactant	50.49±0.15

colon-specific, stable, nanoemulsion-type drug delivery. Further study is required to elucidate the structure–function relationship of this polysaccharide.

## Acknowledgements

We would like to acknowledge CIF, BIT Mesra for providing us with all the analytical data which helped us in every stage of this research.

## Financial support and sponsorship

Nil.

## Conflicts of interest

There are no conflicts of interest.

## REFERENCES

- Kumar M, Bishnoi RS, Shukla AK, Jain CP. Techniques for formulation of nanoemulsion drug delivery system: A review. *Prev Nutr Food Sci* 2019;24:225.
- Gu J, Zhang H, Wen C, Zhang J, He Y, Ma H, *et al.* Purification, characterization, antioxidant and immunological activity of polysaccharide from *Sagittaria sagittifolia* L. *Int Food Res J* 2020;136:109345.
- Ghori MU, Alba K, Smith AM, Conway BR, Kontogiorgos V. Okra extracts in pharmaceutical and food applications. *Food Hydrocoll* 2014;42:342-7.
- Mishra SN, Kumar D, Kumar B, Tiwari S. Assessing impact of varying climatic conditions on distribution of *Buchanania cochinchinensis* in Jharkhand using species distribution modeling approach. *Curr Opin Environ Sustain* 2021;3:100025.
- Ojha AK, Maiti D, Chandra K, Mondal S, Roy DD, Ghosh K, *et al.* Structural assignment of a heteropolysaccharide isolated from the gum of *Cochlospermum religiosum* (Katira gum). *Carbohydr Res* 2008;343:1222-31.
- Bhanja SK, Nandan CK, Mandal S, Bhunia B, Maiti TK, Mondal S, *et al.* Isolation and characterization of the immunostimulating  $\beta$ -glucans of an edible mushroom *Termitomyces robustus* var. *Carbohydr Res* 2012;357:83-9.
- Varma CA, Panpalia SG, Kumar KJ. Physicochemical and release kinetics of natural and retrograded starch of Indian palmyrah shoots. *Int J Biol Macromol* 2014;66:33-9.
- Olayinka OO, Adebowale KO, Olu-Owolabi IB. Physicochemical properties, morphological and X-ray pattern of chemically modified white sorghum starch. (Bicolor-Moench). *J Food Sci Technol* 2013;50:70-7.
- Deepika V, Kumar KJ, Anima P. Isolation and physicochemical characterization of sustained releasing starches from Dioscorea of Jharkhand. *Int J Biol Macromol* 2013;55:193-200.
- Shahidi F, Han XQ, Synowiecki J. Production and characteristics of protein hydrolysates from capelin (*Mallotus villosus*). *Food Chem* 1995;53:285-93.
- Varma CA, Kumar KJ. Structural, functional and pH sensitive release characteristics of water-soluble polysaccharide from the seeds of *Albizia lebbek* L. *Carbohydr Polym* 2017;175:502-8.
- Rahim N, Li AR, Kamarun D, Ahmad MR. Isolation and characterization of galactomannan from seed of *Leucaena leucocephala*. *Polym Bull* 2018;75:2027-37.
- Molaei H, Jahanbin K. Structural features of a new water-soluble polysaccharide from the gum exudates of *Amygdalus scoparia* Spach (Zedo gum). *Carbohydr Polym* 2018;182:98-105.
- Ruiz-Matute AI, Hernández-Hernández O, Rodríguez-Sánchez S, Sanz ML, Martínez-Castro I. Derivatization of carbohydrates for GC and GC-MS analyses. *J Chromatogr B* 2011;879:1226-40.
- Rout D, Mondal S, Chakraborty I, Islam SS. The structure of a polysaccharide from Fraction-II of an edible mushroom, *Pleurotus florida*. *Carbohydr Res* 2006;341:995-1002.
- Sahragard N, Jahanbin K. Structural elucidation of the main water-soluble polysaccharide from *Rubus anatolicus* roots. *Carbohydr Polym* 2017;175:610-7.
- Azeem A, Rizwan M, Ahmad FJ, Iqbal Z, Khar RK, Aqil M, *et al.* Nanoemulsion components screening and selection: A technical note. *AAPS PharmSciTech* 2009;10:69-76.
- Acharya U, Rajarajan S, Acharya R, Acharya R, Chaudhary G, Ghimire S. Formulation and evaluation of nano emulsion-based system for transdermal delivery of antipsoriatic drug. *World J Pharm Sci* 2017;6:732-48.
- Ghosh V, Mukherjee A, Chandrasekaran N. Ultrasonic emulsification of food-grade nanoemulsion formulation and evaluation of its bactericidal activity. *Ultrason Sonochem* 2013;20:338-44.
- Yin B, Deng W, Xu K, Huang L, Yao P. Stable nano-sized emulsions produced from soy protein and soy polysaccharide complexes. *J Colloid Interface Sci* 2012;380:51-9.
- Liu F, Wang D, Sun C, Gao Y. Influence of polysaccharides on the physicochemical properties



- of lactoferrin–polyphenol conjugates coated  $\beta$ -carotene emulsions. *Food Hydrocoll* 2016;52:661-9.
22. Li Q, Wang Z, Dai C, Wang Y, Chen W, Ju X, *et al.* Physical stability and microstructure of rapeseed protein isolate/gum Arabic stabilized emulsions at alkaline pH. *Food Hydrocoll* 2019;88:50-7.
23. Martin-Piñero MJ, García MC, Muñoz J, Alfaro-Rodríguez MC. Influence of the welan gum biopolymer concentration on the rheological properties, droplet size distribution and physical stability of thyme oil/W emulsions. *Int J Biol Macromol* 2019;133:270-7.
24. Md S, Alhakamy NA, Aldawsari HM, Husain M, Kotta S, Abdullah ST, *et al.* Formulation design, statistical optimization, and *in vitro* evaluation of a naringenin nanoemulsion to enhance apoptotic activity in a549 lung cancer cells. *Pharmaceuticals* 2020;13:152.
25. Rachmawati H, Budiputra DK, Mauludin R. Curcumin nanoemulsion for transdermal application: Formulation and evaluation. *Drug Dev Ind Pharm* 2015;41:560-6.
26. Suvakanta D, Narsimha MP, Pulak D, Joshabir C, Biswajit D. Optimization and characterization of purified polysaccharide from *Musa sapientum* L. as a pharmaceutical excipient. *Food Chem* 2014;149:76-83.
27. Bagchi S, Kumar KJ. Studies on water soluble polysaccharides from *Pithecellobium dulce* (Roxb.) Benth. seeds. *Carbohydr Polym* 2016;138:215-21.
28. Kolsi RB, Fakhfakh J, Krichen F, Jribi I, Chiarore A, Patti FP, *et al.* Structural characterization and functional properties of antihypertensive *Cymodocea nodosa* sulfated polysaccharide. *Carbohydr Polym* 2016;151:511-22.
29. Akbari-Alavijeh S, Soleimani-Zad S, Sheikh-Zeinoddin M, Hashmi S. Pistachio hull water-soluble polysaccharides as a novel prebiotic agent. *Int J Biol Macromol* 2018;107:808-16.
30. Kusumayanti H, Handayani NA, Santosa H. Swelling power and water solubility of cassava and sweet potatoes flour. *Procedia Environ Sci* 2015;23:164-7.
31. Munir H, Shahid M, Anjum F, Mudgil D. Structural, thermal and rheological characterization of modified *Dalbergia sissoo* gum—A medicinal gum. *Int J Biol Macromol* 2016;84:236-45.
32. Archana G, Sabina K, Babuskin S, Radhakrishnan K, Fayidh MA, Babu PA, *et al.* Preparation and characterization of mucilage polysaccharide for biomedical applications. *Carbohydr Polym* 2013;98:89-94.
33. Zhi F, Yang TL, Wang Q, Jiang B, Wang ZP, Zhang J, *et al.* Isolation, structure and activity of a novel water-soluble polysaccharide from *Dioscorea opposita* Thunb. *Int J Biol Macromol* 2019;133:1201-9.
34. Wang KP, Wang J, Li Q, Zhang QL, You RX, Cheng Y, *et al.* Structural differences and conformational characterization of five bioactive polysaccharides from *Lentinus edodes*. *Food Res Int* 2014;62:223-32.
35. Chien RC, Yen MT, Tseng YH, Mau JL. Chemical characteristics and anti-proliferation activities of *Ganoderma tsugae* polysaccharides. *Carbohydr Polym* 2015;128:90-8.
36. Nandan CK, Sarkar R, Bhanja SK, Mondal S, Islam SS. Structural characterization of a heteropolysaccharide isolated from the rhizomes of *Curcuma zedoaria* (Sati). *Carbohydr Polym* 2011;86:1252-9.
37. Zou P, Yang X, Huang WW, Zhao HT, Wang J, Xu RB, *et al.* Characterization and bioactivity of polysaccharides obtained from pine cones of *Pinus koraiensis* by graded ethanol precipitation. *Molecules* 2013;18:9933-48.
38. Jahanbin K, Abbasian A, Ahang M. Isolation, purification and structural characterization of a new water-soluble polysaccharide from *Eremurus stenophyllus* (boiss. & buhse) baker roots. *Carbohydr Polym* 2017;178:386-93.
39. Zou YF, Zhang YY, Paulsen BS, Rise F, Chen ZL, Jia RY, *et al.* Structural features of pectic polysaccharides from stems of two species of *Radix Codonopsis* and their antioxidant activities. *Int J Biol Macromol* 2020;159:704-13.
40. Pinto M, Coelho E, Nunes A, Brandão T, Coimbra MA. Valuation of brewers spent yeast polysaccharides: A structural characterization approach. *Carbohydr Polym* 2015;116:215-22.
41. Farhadi N. Structural elucidation of a water-soluble polysaccharide isolated from Balangu shirazi (*Lallemantia royleana*) seeds. *Food Hydrocoll* 2017;72:263-70.
42. Rodrigues DC, Cunha AP, Brito ES, Azeredo HM, Gallao MI. Mesquite seed gum and palm fruit oil emulsion edible films: Influence of oil content and sonication. *Food Hydrocoll* 2016;56:227-35.
43. Chivero P, Gohtani S, Yoshii H, Nakamura A. Physical properties of oil-in-water emulsions as a function of oil and soy soluble polysaccharide types. *Food Hydrocoll* 2014;39:34-40.
44. Jafari E. Preparation, characterization and dissolution of solid dispersion of diclofenac sodium using Eudragit E-100J. *App Pharm Sci* 2013;3:167.
45. Zeng L, Liu Y, Pan J, Liu X. Formulation and evaluation of norcanthridin nanoemulsions against the *Plutella xylostella* (Lepidoptera: Plutellidae). *BMC Biotech* 2019;19:16.
46. Matos M, Marefati A, Bordes R, Gutiérrez G, Rayner M. Combined emulsifying capacity of polysaccharide particles of different size and shape. *Carbohydr Polym* 2017;169:127-38.
47. Chivero P, Gohtani S, Yoshii H, Nakamura A. Effect of xanthan and guar gums on the formation and stability of soy soluble polysaccharide oil-in-water emulsions. *Food Res Int* 2015;70:7-14.
48. Castel V, Rubiolo AC, Carrara CR. Improvement of emulsifying properties of Brea gum by controlled thermal treatment. *Food Hydrocoll* 2018;85:93-101.
49. Pérez-Mosqueda LM, Trujillo-Cayado LA, Carrillo F, Ramírez P, Muñoz J. Formulation and optimization by experimental design of eco-friendly emulsions based on d-limonene. *Colloids Surf B Biointerfaces* 2015;128:127-31.
50. Thakkar HP, Khunt A, Dhande RD, Patel AA. Formulation and evaluation of Itraconazole nanoemulsion for enhanced oral bioavailability. *J Microencapsul* 2015;32:559-69.